

Phenylglycine and phenylalanine derivatives as potent and selective HDAC1 inhibitors (SHI-1)

Kevin J. Wilson,^{a,*} David J. Witter,^a Jonathan B. Grimm,^a Phieng Siliphaivanh,^a Karin M. Otte,^a Astrid M. Kral,^b Judith C. Fleming,^b Andreas Harsch,^a Julie E. Hamill,^a Jonathan C. Cruz,^c Melissa Chenard,^c Alexander A. Szewczak,^a Richard E. Middleton,^a Bethany L. Hughes,^a William K. Dahlberg,^a J. Paul Secrist^b and Thomas A. Miller^a

^aDepartment of Drug Design and Optimization, Merck Research Laboratories, 33 Avenue Louis Pasteur, Boston, MA 02115, USA

^bDepartment of Cancer Biology and Therapeutics, Merck Research Laboratories, 33 Avenue Louis Pasteur, Boston, MA 02115, USA

^cDepartment of Oncology Pharmacology, Merck Research Laboratories, 33 Avenue Louis Pasteur, Boston, MA 02115, USA

Received 2 January 2008; revised 7 February 2008; accepted 7 February 2008

Available online 10 February 2008

Abstract—An HTS screening campaign identified a series of low molecular weight phenols that showed excellent selectivity (>100-fold) for HDAC1/HDAC2 over other Class I and Class II HDACs. Evolution and optimization of this HTS hit series provided HDAC1-selective (SHI-1) compounds with excellent anti-proliferative activity and improved physical properties. Dose-dependent efficacy in a mouse HCT116 xenograft model was demonstrated with a phenylglycine SHI-1 analog.

© 2008 Elsevier Ltd. All rights reserved.

Ongoing clinical studies with histone deacetylase (HDAC) inhibitors indicate that these agents show great promise for the treatment of cancer.¹ Zolinza® (SAHA, vorinostat), belonging to the hydroxamic acid class of HDAC inhibitors, represents the first of these to gain approval by the FDA.² Following this success, there remains significant interest in identifying HDAC inhibitors with improved efficacy and tolerability. With this in mind, we sought to identify compounds with increased HDAC isoform specificity. An HTS screening campaign identified a series of low molecular weight phenols, typified by compound **1** (Fig. 1), bearing a novel biaryl motif in the zinc binding region of the HDAC inhibitor pharmacophore.³ The biaryl unit was found to impart excellent selectivity (>100-fold) for Class I HDACs 1 and 2 over other Class I HDACs (3 and 8) and Class II HDACs (4–7).⁴

HTS screening hit **1** showed moderately potent inhibition of both the HDAC1 isoform and proliferation of the human colon carcinoma cell line HCT116.⁵ Combining our newly discovered biaryl unit with a truncated

version of the *N*-(2-aminophenyl)benzamide scaffold^{6,7} provided hybrid compound **2** (Fig. 1). This transformation had no effect on enzymatic or cell-based potency. However, replacing the pendant phenyl ring with the isosteric 2-thienyl unit⁸ (**3**) enhanced anti-proliferative activity relative to phenol **1**, although no change in HDAC1 inhibitory potency was observed. Biaryl benzamide **3**, thus derived from an HTS screening lead, represented an excellent starting point for further medicinal chemistry optimization.

Compound **3** was found to possess sub-optimal physical properties, with very poor aqueous solubility (0 nM at pH 7) and a moderate log *D*₇ of 2.7.⁹ We reasoned that the addition of an amino acid-derived substituent to the core scaffold would increase polarity and improve aqueous solubility. We targeted the 4-position of the benzamide core following our recent success with both amino acid-⁶ and malonyl-derived⁷ benzamide HDAC inhibitors (Fig. 1). Our goal was to establish the minimum structural elements required for potent inhibition of HDAC1 and cell proliferation while obtaining suitable physical properties.

We began our investigation by synthesizing parent phenylglycine analog **4** bearing a free amino acid group, as outlined in Scheme 1. Palladium coupling of *tert*-bu-

Keywords: HDAC1 inhibitor; Selective; Biaryl; Benzamide.

*Corresponding author. Tel.: +1 617 992 2066; fax: +1 617 992 2403; e-mail: kevin_wilson2@merck.com

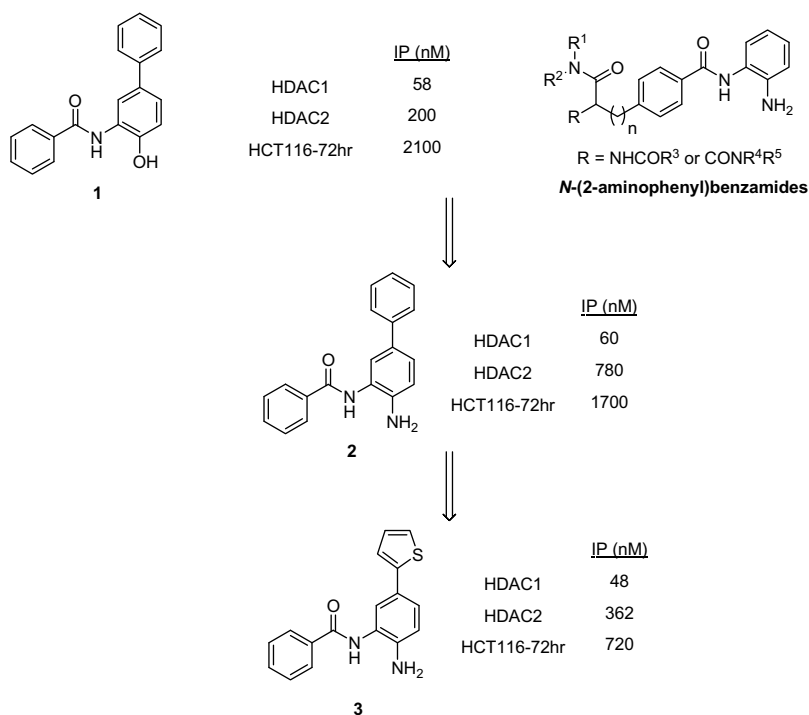
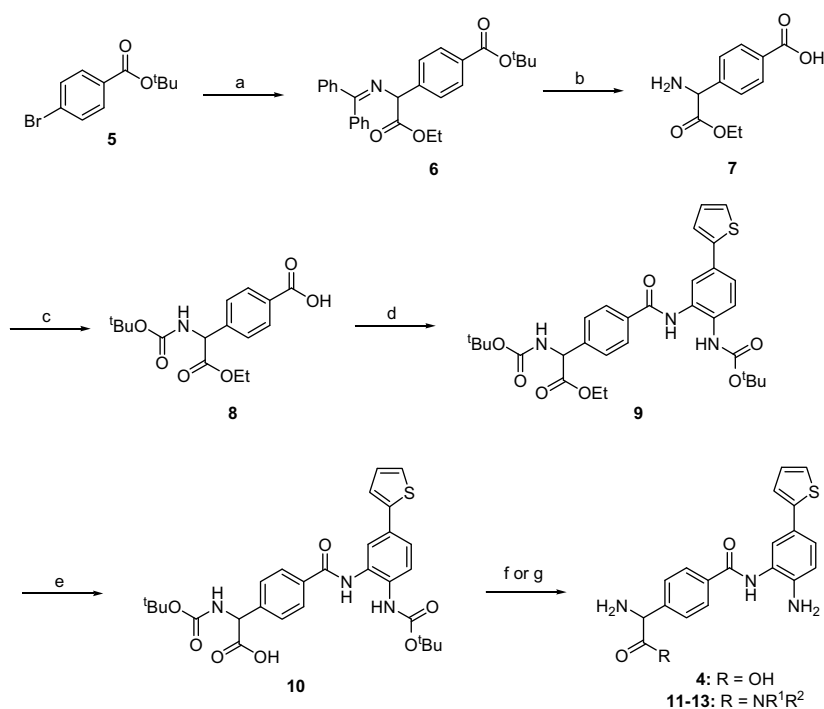


Figure 1. HDAC1 and proliferation inhibitory potency of a biaryl phenol HTS screening hit (**1**), related aniline derivatives (**2** and **3**) and representative *N*-(2-aminophenyl)benzamides. IP, inflection point.

tyl 4-bromobenzoate **5** with ethyl [(diphenylmethylidene)amino]acetate¹⁰ gave protected amino di-ester **6**. Acid hydrolysis of both the *tert*-butyl ester and imine provided amino ester substituted benzoic acid **7**. The

free amine was first protected (**8**) before adding the biaryl head group³ via a Bop coupling to provide benzamide **9**. Hydrolysis of the ethyl ester yielded advanced carboxylic acid **10**. Finally, concomitant removal of both Boc



Scheme 1. Reagents and conditions: (a) ethyl [(diphenylmethylidene)amino]acetate, K₃PO₄, Pd(P^tBu₃)₂, 100 °C; (b) 2 N HCl, Et₂O; (c) Boc₂O, DIPEA, THF; (d) 1,1-dimethylethyl [2-amino-4-(2-thienyl)phenyl]carbamate, BOP, DIPEA, DMF; (e) 1 N LiOH, THF; (f) TFA, DCM, (g) i—Amine·HCl, EDC, HOBT, DIPEA, DMF; ii—TFA, DCM.

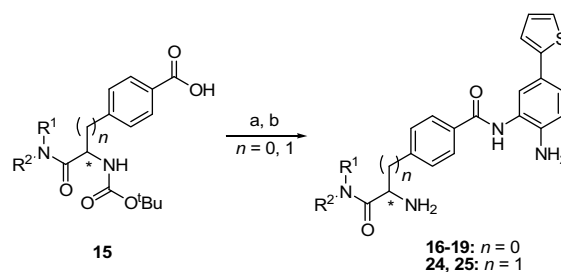
groups according to standard conditions yielded desired amino acid **4**.

The addition of the amino acid unit maintained equivalent HDAC1 inhibitory potency relative to **3** (Table 1). However, amino acid **4** lacked cell proliferation inhibition activity, which is most likely a reflection of the poor membrane permeability of the zwitterion. Reasoning that cell-based potency could be improved by converting the acid to more cell penetrant functionalities, we undertook the SAR evaluation of amide derivatives. In order to minimize molecular weight, we chose to synthesize a small series of minimally substituted amides, that is, NH₂, NHMe, and NMe₂. To this end, **10** proved to be a useful intermediate allowing access to these amides via a routine EDC coupling followed by removal of the Boc groups under acidic conditions (Scheme 1).¹¹

An increase in HDAC1 inhibition was observed for all amide analogs relative to the acid, ranging from sixfold for methyl amide **12** and dimethyl amide **13** to 10-fold for primary amide **11**. Gratifyingly, the amides possessed excellent anti-proliferative activity showing a twofold improvement over the unsubstituted compound **3** (Table 1). Interesting SAR was observed with respect to hERG binding.¹² The more lipophilic dimethylamide **13** possessed a moderate degree of affinity for this ion channel (IC₅₀ = 6.8 μM). hERG affinity was significantly reduced with the more polar primary and methyl amides (<20% inhibition at 10 μM). The ethyl ester **14**¹³ further illustrates this trend, being both the most lipophilic and the most potent hERG ligand (IC₅₀ = 5.7 μM) within this series.¹⁴ In addition to their excellent HDAC1 and proliferation inhibition properties, the amino amides exhibited favorable physical

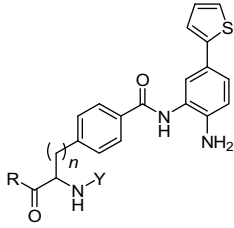
properties. Representative analogs **11** and **12** possessed log *D*₇ values of 1.49 and 1.57, respectively, with the aqueous solubility (pH 7) of both compounds around 185 μM.

Further optimization of this series of novel, low molecular weight HDAC1 inhibitors included the evaluation of individual enantiomers. For this purpose, we developed a synthesis of chiral benzoic acid derivatives **15** from the commercially available enantiomers of 4-hydroxyphenylglycine.¹⁵ The key step in this sequence was the carbonylation of an aryl triflate, which required the use of DIPEA rather than TEA to suppress racemization of the stereochemistry. Both enantiomers of the primary amide (**16** and **17**) and methylamide (**18** and **19**) were readily accessed from these chiral benzoates via a Bop coupling to install the biaryl head-group followed by TFA-mediated deprotection (Scheme 2, *n* = 0). No stereochemical preference was observed with respect to inhibition of either HDAC1 or cell proliferation (Table 1).



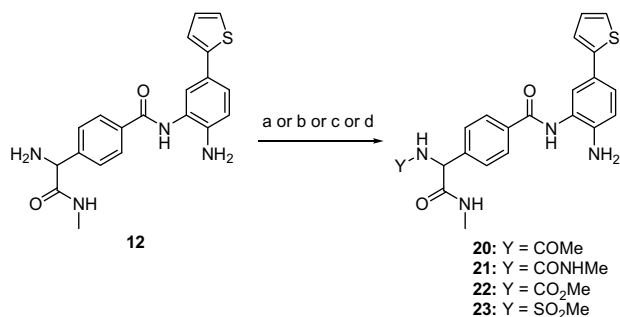
Scheme 2. Reagents: (a) 1,1-dimethylethyl [2-amino-4-(2-thienyl)phenyl]carbamate, BOP, DIPEA, DMF; (b) TFA, DCM.

Table 1.



Compound	R	Y	<i>n</i>	HDAC1 IP ^a (nM)	HCT116-72 h IP ^a (nM)
4	OH	H	0	66	>20,000
11	NH ₂	H	0	5.7	350
12	NHMe	H	0	10	450
13	NMe ₂	H	0	8.8	420
14	OEt	H	0	10	1100
16	NH ₂ (<i>R</i>)	H	0	12	350
17	NH ₂ (<i>S</i>)	H	0	11	510
18	NHMe (<i>R</i>)	H	0	14	420
19	NHMe (<i>S</i>)	H	0	22	480
20	NHMe	COMe	0	14	620
21	NHMe	CONHMe	0	10	960
22	NHMe	CO ₂ Me	0	18	410
23	NHMe	SO ₂ Me	0	29	780
24	NH ₂ (<i>R</i>)	H	1	37	390
25	NH ₂ (<i>S</i>)	H	1	29	260

^a Values are means of *n* ≥ 2.



Scheme 3. Reagents: (a) Y = COMe: Ac_2O , DIPEA, THF; (b) Y = CONHMe: MeNCO , THF; (c) Y = CO_2Me : ClCO_2Me , DIPEA, THF; (d) Y = SO_2Me : MeSO_2Cl , DIPEA, THF.

Having established that low molecular weight phenylglycine derivatives **11**–**19** were potent inhibitors of HDAC1 and cell proliferation, we next wished to assess the effect of additional modifications. To this end, the primary amine of **12** was selectively capped by reacting with various electrophiles (Scheme 3). Acetamide **20** and methyl urea **21** exhibited equipotent inhibition of HDAC1 relative to **12**, whereas the methyl carbamate **22** and methyl sulfonamide **23** showed a two- and threefold loss of potency, respectively. Only **22** retained equivalent inhibition of cell proliferation, with all other analogs showing attenuated cell-based potencies (Table 1).

We also extended our investigation to include phenylalanine homologs, exemplified by primary amides **24** and **25**. These analogs were readily accessed from chiral benzoates **15** ($n = 1$) according to Scheme 2. These enantiomerically pure building blocks were again synthesized via an hydroxycarbonylation approach, this time employing triflates derived from L- or D-tyrosine.¹⁵ Both enantiomers showed a three- to fourfold decrease in HDAC1 inhibition relative to the lower homologs ($n = 0$) but maintained equivalent anti-proliferative potency (Table 1). Adding additional molecular weight, either through derivatizing the amino unit or adding larger amide substituents, provided analogs with comparable HDAC1 inhibitory potency in both the phenylglycine and phenylalanine homologs. However, these larger derivatives suffered from increased hERG binding and offered no advantage with respect to pharmacokinetics or other properties (data not shown).

Having identified potent inhibitors of the HDAC1 isoform and cell proliferation, we profiled this series against additional HDAC isoforms. As with the unsubstituted benzamide **3**, representative analog **12** exhibited excellent HDAC1 selectivity, ranging from 13-fold relative to HDAC2, 350-fold relative to HDAC3 and HDAC11, and ≥ 3500 -fold over the remaining isoforms

(Table 2).¹⁶ The unique selectivity profile of this new class of inhibitors arises from the addition of the second aryl group on to the zinc binding diamine. One possible explanation is that the pendant aryl ring is able to occupy the internal cavity¹⁷ within HDAC1 but not the internal cavity of other isoforms, thus imparting potency and selectivity for this isoform.³

Based on the excellent in vitro profile of compound **12**, pharmacokinetic parameters were determined in multiple species (Table 3). This analog exhibited moderate (rat) to low (dog and rhesus) plasma clearance with an acceptable half-life in rat and dog. The half-life in rhesus was found to be shorter as a result of a reduced volume of distribution in this species. Oral bioavailability was satisfactory in rat but lower in dog and very poor in rhesus.

Despite the sub-optimal pharmacokinetic profile, we chose to further characterize methyl amide **12** in a 21-day HCT116 mouse xenograft study. Gratifyingly, **12** exhibited dose-dependent tumor growth inhibition (TGI) following ip administration (Fig. 2). A dose of 65 mg/kg qd was sufficient to produce TGI equivalent to vorinostat (150 mg/kg ip qd). These data provide evidence of the utility of our selective HDAC1 inhibitors as potential anti-cancer therapeutics.

In conclusion, the evolution and optimization of a novel scaffold identified by HTS yielded compounds with excellent inhibitory potency of HDAC1 and cell proliferation. The presence of a biaryl unit in the zinc binding domain was found to impart a high degree of selectivity for HDAC1 over other Class I and Class II isoforms. The strategy of appending amino acid-derived substituents was successful in improving aqueous solubility (e.g. 185 μM at pH 7 for compounds **11**, **12**, and **24**) while minimizing off-target activity. Efficacy was demonstrated in a mouse xenograft model despite sub-optimal pharmacokinetic properties. Further optimization and characterization of biaryl SHI-1 will be the subject of subsequent publications.

Table 3. PK parameters for compound **12**

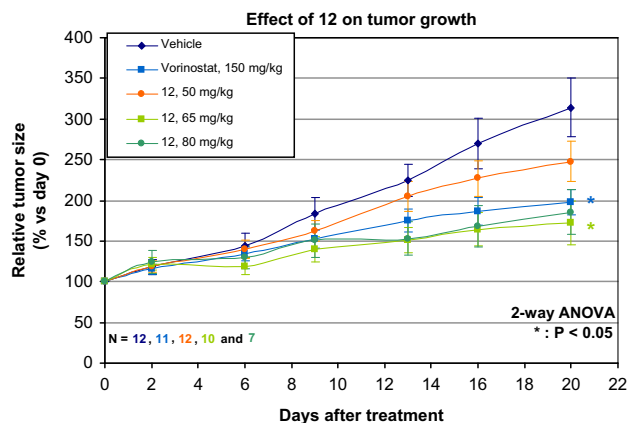
Species	IV AUC ($\mu\text{M h kg/mg}$)	Cl (mL/min/kg)	V_{dss} (L/kg)	$T_{1/2}$ (h)	F (%)
Rat ^a	1.2	38	7.6	5.9	27
Dog ^b	4.0	11	3.2	5.4	17
Rhesus ^b	2.7	16	1.6	1.6	5

^a IV dose 2 mg/kg, oral dose 4 mg/kg.

^b IV dose 0.5 mg/kg, oral dose 1 mg/kg.

Table 2. Compound **12** HDAC isoform selectivity profile

	HDAC1	HDAC2	HDAC3	HDAC4	HDAC5	HDAC6	HDAC7	HDAC8	HDAC11
IP (nM)	10	130	3400	>50,000	>50,000	>50,000	>50,000	35,000	3600
Fold sel.	—	13×	340×	>5000×	>5000×	>5000×	>5000×	3500×	360×



Plasma concentrations of 12:

	50 mg/kg	65 mg/kg	80 mg/kg
2 hr	17.9 μ M	28.6 μ M	nd
4 hr	4.1 μ M	10.0 μ M	nd
24 hr	0.01 μ M	0.02 μ M	nd

Figure 2. 21-day mouse xenograft data and corresponding plasma exposures. nd, not determined.

Acknowledgments

We wish to thank Xiaoliu Geng and Adam Beard for the solubility and log D_7 determinations.

References and notes

- Glaser, K. B. *Biochem. Pharm.* **2007**, *74*, 659.
- Grant, S.; Easley, C.; Kirkpatrick, P. *Nat. Rev. Drug Disc.* **2007**, *6*, 21.
- Witter, D. J.; Harrington, P.; Wilson, K. J.; Chenard, M.; Cruz, J. C.; Fleming, J. C.; Harsch, A.; Kral, A. M.; Secrist, J. P.; Miller, T. A. *Bioorg. Med. Chem. Lett.* **2008**, *18*, 726.
- For assay details, see reference within Jones, P.; Altamura, S.; Chakravarty, P. K.; Cecchetti, O.; De Francesco, R.; Gallinari, P.; Ingenito, R.; Meinke, P. T.; Petrocchi, A.; Rowley, M.; Scarpelli, R.; Serafini, S.; Steinkühler, C. *Bioorg. Med. Chem. Lett.* **2006**, *16*, 5948–5952.
- For assay details, see Ref. 3.
- Hubbs, J. L.; Zhou, H.; Kral, A. M.; Fleming, J. C.; Dahlberg, W. K.; Hughes, B. L.; Middleton, R. E.; Szwczak, A. A.; Secrist, P.; Miller, T. A. *Bioorg. Med. Chem. Lett.* **2008**, *18*, 34.
- Siliphaivanh, P.; Harrington, P.; Witter, D. J.; Otte, K.; Tempest, P.; Kattar, S.; Kral, A. M.; Fleming, J. C.; Deshmukh, S. V.; Harsch, A.; Secrist, P.; Miller, T. A. *Bioorg. Med. Chem. Lett.* **2007**, *17*, 4619.

- During the preparation of this manuscript a report describing the 2-thienyl head-group was published: Moradei, O. M.; Mallais, T. C.; Frechette, S.; Paquin, I.; Tessier, P. E.; Leit, S. M.; Fournal, M.; Bonfils, C.; Trachy-Bourget, M.-C.; Liu, J.; Yan, T. P.; Lu, A.-H.; Rahil, J.; Wang, J.; Lefebvre, S.; Li, Z.; Vaisburg, A. F.; Besterman, J. M. *J. Med. Chem.* **2007**, *50*, 5543.
- Aqueous solubility and log D_7 values were determined using a high-throughput HPLC assay. For this assay two samples were prepared: one 100 μ M solution in organic solvent (8:1:1, MeOH:MeCN:DMSO) and one 200 μ M solution in PBS buffered water at pH 7. The sample in PBS buffered water was agitated for 24 h at room temperature and filtered to remove any compound that had precipitated. The sample in organic solvent was fully dissolved. Both the sample in organic solvent and the filtered supernatant of the sample in PBS buffered water were run using the same HPLC method and the areas of the compound peaks for each sample were compared in order to determine the concentration of compound dissolved in PBS buffered water. This concentration indicated the solubility of the compound in water up to a maximum concentration of 200 μ M. To determine log D_7 for the compound, several standards with known log D_7 values were run using the same HPLC method and a standard curve was generated that related log D_7 to retention time. The retention time of the compound peak from the sample dissolved in organic solvent was then used with the equation for the best fit line of the log D_7 standard curve to determine the log D_7 value for the compound.
- Lee, S.; Beare, N. A.; Hartwig, J. F. *J. Am. Chem. Soc.* **2001**, *123*, 8410.
- Spectral data for the TFA salt of representative amino amide **12**: ^1H NMR (DMSO- d_6 , 600 MHz) δ 9.83 (s, 1H), 8.72 (br s, 3H), 8.50 (q, J = 4.2 Hz, 1H), 8.04 (d, J = 8.4 Hz, 2H), 7.61 (d, J = 8.4 Hz, 2H), 7.47 (d, J = 1.2 Hz, 1H), 7.35 (d, J = 4.8 Hz, 1H), 7.32 (dd, J = 8.1 and 2.1 Hz, 1H), 7.24 (d, J = 3.6 Hz, 1H), 7.03 (dd, J = 4.8 and 3.6 Hz, 1H), 6.84 (d, J = 8.4 Hz, 1H), 4.97 (br s, 1H), 2.61 (d, J = 4.2 Hz, 3H). MS: calc'd 381 (MH $^+$), exp 381 (MH $^+$). For full experimental details, see WO2007100657.
- For assay details, see Wang, J.; Della Penna, K.; Wang, H.; Karczewski, J.; Connolly, T. M.; Koblan, K. S.; Bennett, P. B.; Salata, J. J. *Am. J. Physiol.* **2003**, *284*, H256.
- Synthesized by treating compound **9** with TFA in DCM.
- For a review of hERG optimizations, including a discussion of the effect of lipophilicity, see Jamieson, C.; Moir, E. M.; Rankovic, Z.; Wishart, G. *J. Med. Chem.* **2006**, *49*, 5029.
- Grimm, J. B.; Wilson, K. J.; Witter, D. J. *Tetrahedron Lett.* **2007**, *48*, 4509.
- Relative HDAC1 selectivity values were consistent across all analogs discussed herein.
- Wang, D.; Wiest, O.; Helquist, P.; Lan-Hargest, H.; Wiech, N. L. *J. Med. Chem.* **2004**, *47*, 3409.